8. THE OBSERVATION PROGRAMME AND INTERFACE WITH THE INPUT CATALOGUE CONSORTIUM

This chapter describes the manner in which the satellite scanned the sky (the ecliptic-based scanning law). This scanning law ensured even coverage of the sky during the mission lifetime. The observation programme was nominally fixed before satellite launch, and the entire satellite operations and scientific observations were conducted on the basis of the pre-defined Hipparcos Input Catalogue. Nevertheless, considerable 'tuning' of the observing programme went on throughout the mission, especially during the early months of the mission. Very few objects had significantly erroneous positions or magnitudes, which were duly corrected as they became evident. Several updates of the global positions were made on the basis of the early data reductions, in order to improve the real-time attitude determination performances, and resulting photometric measurements. The parameters of the global observing programme were also adjusted throughout the mission taking into account the past and future (expected) observation times allocated to each object. The way in which the star observations were carried out—by interlacing observations of all stars simultaneously present in the combined field of view of the telescope—is described. Predicted appearances of the individual stars were computed on ground, on the basis of the Hipparcos Input Catalogue, and target observation times were pre-computed, based on the star's magnitude and priority and, ultimately, on the previous observing history of the star.

8.1. Scanning Law

Scanning Law Definition

Each object in the Hipparcos Input Catalogue was scheduled to be observed many times with different scanning orientations (typically some 100 times, although this varied considerably according principally to the object's ecliptic latitude) to increase the accuracy and precision of the parameters which would constitute the end results of the mission. This was achieved by constraining the attitude of the spacecraft to follow a complex 'revolving scanning' motion, called the nominal scanning law, which ensured reasonably even coverage of the sky over the lifetime of the mission whilst adhering

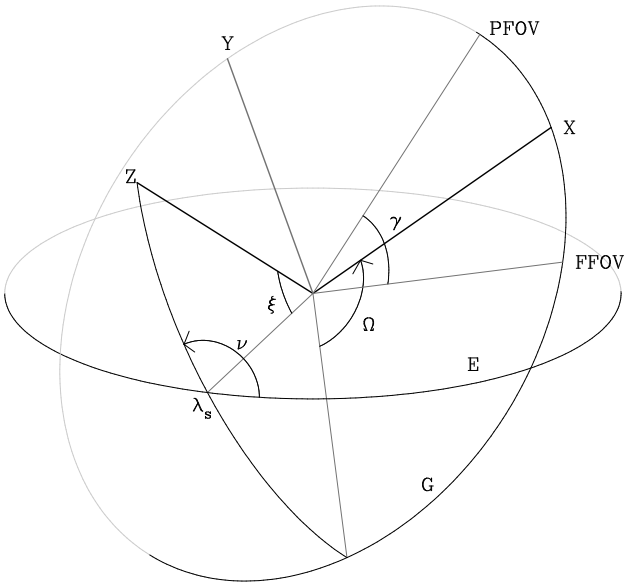

Figure 8.1. *Definition of the telescope reference frame (X, Y, Z). The spin axis of the satellite, Z, precessed around the sun line at a constant inclination angle of $\xi = 43°$, with the satellite rotating around this axis at a rate of R = 11.25 revolutions per day. E signifies the ecliptic plane, and λ_S the ecliptic latitude of the Sun. The precession angle, ν, and the heliotropic angle, Ω, define the elements of the scanning law through Equation 8.8. PFOV and FFOV refer to the preceding and following fields of view; G is the scanning great circle, and γ is the 'basic angle' between the two viewing directions.*

to thermal and other constraints. Three-axis control of the spacecraft was performed by regular firings of cold-gas thrusters (approximately every 10 min). In this way, the spacecraft rotated at 168°.75 per hour about its principal rotation axis, which itself was constrained to precess at roughly 6°.3 per day about a 43° half-cone centred on the Sun direction. It should be noted that the principles of the nominal scanning law, and of the programme star file and the star observing strategy, were not affected by the revised orbit.

The satellite attitude motion was most easily described in terms of the movement of the telescope with respect to the ecliptic reference system. The telescope reference frame (Figure 8.1) is the rectangular right-handed frame (OXYZ), where the origin, O, is the intersection of the two lines of sight, OP and OF, of the telescope; the plane (X,Y) is coincident with the plane (P,F); and the X-axis is the bisector of the basic angle POF. The satellite scanning motion was then defined as follows: the Z-axis of the telescope reference frame rotated at a constant angle $\xi = 43°$ around the Sun direction, following the Sun in its apparent motion along the ecliptic and performing $K = 6.4$ revolutions per year. At the same time, the satellite rotated around the Z-axis in the (X,Y)-plane performing $R = 11.25$ revolutions per day. The motions of the axes OP and OF of the preceding and following fields of view, which scanned the celestial sphere, resulted directly from this scanning motion.

Quantitative Description of the Scanning Law

In precise terms, the nominal sun line is defined by the following orientation:

$$\mathbf{s}(d) = \mathbf{l}\cos\lambda_s + \mathbf{j}\sin\lambda_s \qquad [8.1]$$

l j k being the ecliptic coordinate triad for the mean ecliptic and equinox of J2000.0, and:

$$\lambda_s = L + 2e\sin g + \frac{5}{4}e^2\sin 2g \qquad [8.2]$$

$$L = -1.386\,91 + 0.017\,202\,124\,0d \qquad [8.3]$$

$$g = -0.041\,14 + 0.017\,201\,969\,6d \qquad [8.4]$$

$$e = +0.016\,714 \qquad [8.5]$$

where d is the time in mean solar days from the reference epoch adopted for the nominal scanning law, defined as 1988 January 1, $12^h00^m00^s$ UTC (in practice, d was defined in terms of the satellite on-board clock).

The composition of the precession of the spin axis Z and the rotation of the Earth (and satellite) around the Sun resulted in a motion of the Z-axis on the celestial sphere, with a speed designated V_Z. The orientation of the telescope reference frame with respect to the heliotropic reference frame was described by the attitude angles v, ξ, Ω. The speed V_Z was kept approximately constant by modulating the precession angle v:

$$v = \overline{v} + a_1\cos(\overline{v}) + a_2\sin(2\overline{v}) + a_3\cos(3\overline{v}) + a_4\sin(4\overline{v}) \qquad [8.6]$$

where $\overline{v} = \overline{v}_0 + 6.4\lambda_s$, and the coefficients a_i are the following:

$$\begin{aligned} a_1 &= -0.163\,784\,59 \\ a_2 &= -0.013\,077\,77 \\ a_3 &= +0.001\,232\,43 \\ a_4 &= +0.000\,123\,41 \end{aligned} \qquad [8.7]$$

The instantaneous spin rate, ω_Z, was kept approximately constant by modulating the heliotropic attitude angle, Ω, as follows:

$$\Omega(d) = \Omega_0 + 2\pi R(d - d_0) - v\cos\xi + (b_1\overline{v} + b_2\cos\overline{v} + b_3\sin(2\overline{v}))\frac{\sin\xi}{K} \qquad [8.8]$$

where:

$$\begin{aligned} b_1 &= +0.082\,152\,69 \\ b_2 &= +0.990\,061\,17 \\ b_3 &= +0.040\,452\,13 \end{aligned} \qquad [8.9]$$

The parameters used in the nominal scanning law were the spin rate, $R = 11.25$ revolutions per day (168.75 arcsec s^{-1}), the revolving scanning angle, $\xi = 43° \pm 0.°5$, and the average precession rate, $K = 6.400 \pm 0.002$ revolutions per year. The principle of the

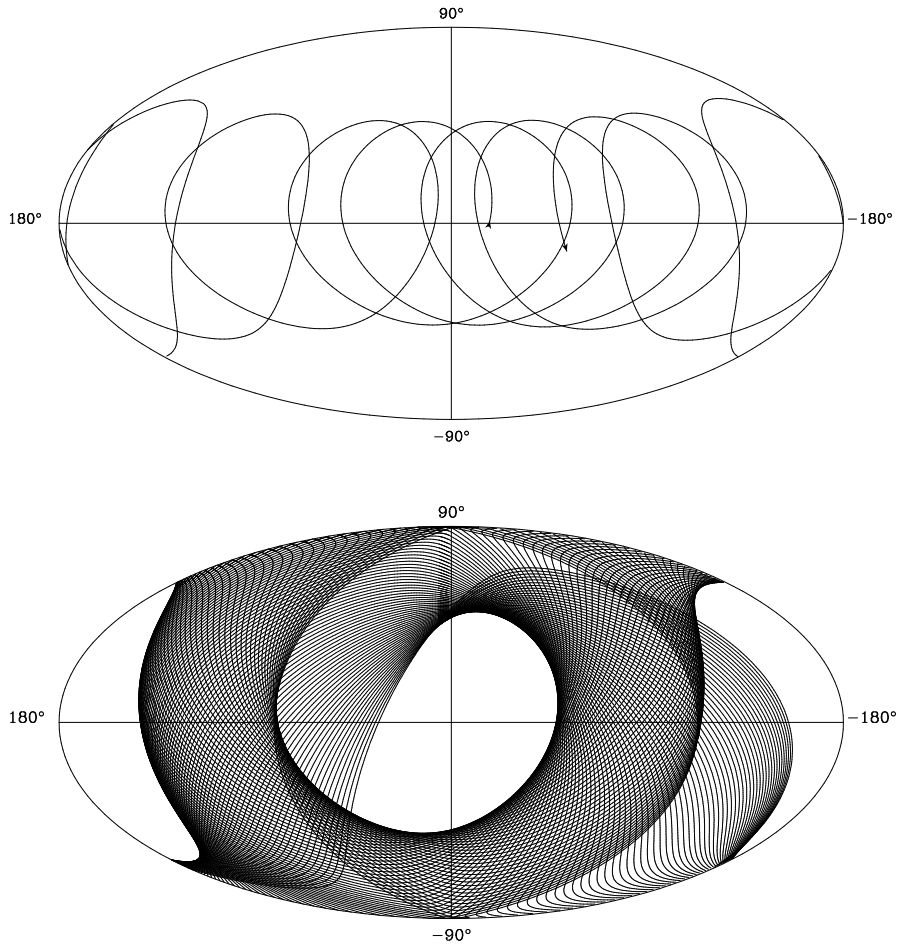

Figure 8.2. *The scanning motion of the Hipparcos satellite on the celestial sphere, shown in ecliptic coordinates. The top figure shows the path of the spin axis between 22 May 1990 and 23 September 1991. The scan direction is indicated by the arrows. The bottom figure shows one reference great circle for each orbit (5 revolutions of the satellite) for the period between 22 May 1990 and 14 July 1990. The actual scanning was 5 times denser.*

scanning measurements is illustrated in Figure 1.1, and the resulting scanning of the celestial sphere is shown in Figure 8.2.

The above description defines the 'nominal scanning law', i.e. the nominal paths of the fields of view on the sky throughout the mission. Deviations of up to ± 10 arcmin about the three satellite axes were tolerated in practice, attitude motion within these limits being controlled autonomously on-board by means of the attitude and orbit control system.

Optional Variations in the Definition

The choice of nominal scanning law parameters had been carefully analysed in the years preceding launch to ensure maximum homogeneity of coverage over the entire sky as well as accuracy of the final catalogue. The results of these studies optimised for the launch data of 8 August 1989, gave values of $\xi = 43°$ and $\overline{v}_0 = 40°$. The value of Ω_0 was less critical and could be defined by ESOC in orbit. The concept employed by ESOC during the commissioning phase after launch was to use the prescribed values of ξ and $\overline{v}_0$ to position the rotation axis of the spacecraft at the correct part of the 43° cone. At that time, using star pattern recognition techniques with the ground real-time attitude determination system, the phase of the fields of view as the spacecraft rotated could be calibrated and hence Ω_0 could be derived.

Although ESOC were in principle able to change the nominal scanning law through the ground software, mission constraints were prescribed which prevented any change to either ξ or $\overline{v}_0$. In addition Ω_0 should only be changed if necessary. Therefore in general, ESOC maintained a constant nominal scanning law throughout the routine (three-gyro) phase of the mission. The only times when it was deemed necessary to change Ω_0 during this period were during a small number of contingencies where the spacecraft assumed a non-nominal spin rate for a significant period of time. In order to re-acquire attitude control, ESOC had the choice of options, either to perform a large firing of the cold gas thrusters to slew the spacecraft around its principal rotation axis thereby re-acquiring the previous nominal scanning law attitude, or to calibrate the value of Ω_0 for the current phase and calculate a new mission plan and programme star file. In all cases where the drift around the rotation axis was more than one or two degrees, the second option was faster to implement, safer and less expensive in fuel.

During the two-gyro operations towards the end of the mission, significant drifts around the rotation axis occurred during every perigee, making re-calibration of Ω_0 necessary every orbit. A full discussion is given in Chapter 15. Moreover, the drifting phase angle also affected the accuracy of the on-board model for the precession around the 43° cone. The result was that the rotation axis itself was prone to drift. ESOC was then faced with a similar but more difficult decision concerning the method of re-acquiring attitude control under these conditions. The options in this case were to perform a large firing of the cold gas thrusters to slew the spin axis back to that position defined by $\overline{v}_0 = 40°$ or to calibrate the value of $\overline{v}_0$ for the current attitude and calculate a new mission plan and programme star file.

The second option was selected for the same reasons as for Ω_0 although it was realised that there may be a penalty to pay in terms of homogeneity of coverage. To monitor any possible biasing, the tables of nominal scanning law parameters used during the mission were monitored by the NDAC Consortium.

During the final brief period of attempted zero-gyro operations, efforts were made to initialise the real-time attitude determination in quasi sun-pointing mode where the solar aspect angle was close to but not exactly zero (see Chapter 16 for a more complete discussion). These attempts were largely unsuccessful, and further attempts were restricted to using a scanning law with $\xi = 0$.

Table 8.1. Nominal scanning law parameters during three-gyro operations.

Start time yy:dd	ξ deg	$\overline{v}_0$ deg	Ω_0 deg
1989:305	43.0	40.0	102.470
1990:178	43.0	40.0	138.850
1990:320	43.0	40.0	135.647
1991:160	43.0	40.0	134.167
1991:279	43.0	40.0	4.566

Table 8.1 lists the nominal scanning law parameters used during the three-gyro operational phase. Figure 8.3 depicts the nominal scanning law parameters for the two-gyro operational phase.

Orbital Oscillator

The nominal body rates of the spacecraft, defined in the nominal scanning law, were modelled on-board as a linear function of parameters referred to as the orbital oscillators S_v, C_v, which modelled the sine and cosine components of the phase angle of the nominal scanning law. The orbital oscillator values were propagated forward in time using an approximate formula, which would have led to a drift from the nominal scanning law unless accurate values were periodically uplinked from ground.

Defining:

Ω_N as the nominal scan rate of $168\overset{\circ}{.}75$ per hour

Ω_p as the precession rate of the spacecraft z-axis around the 43° cone ($\simeq 0\overset{\circ}{.}26$ per hour)

Ω_d as the spin rate accounting for precession ($\simeq 168\overset{\circ}{.}56$ per hour)

Ω_T as the transverse rate

ξ as the solar aspect angle (nominally 43°)

t_k as the on-board time sampled every $\Delta t = \frac{16}{15}$ seconds

$\Omega_N, \Omega_p, \Omega_d, \Omega_T$ were related via the equations:

$$\begin{aligned} \Omega_T &= \Omega_P \sin \xi \\ \Omega_N &= \Omega_P \cos \xi + \Omega_d \end{aligned} \qquad [8.10]$$

$S_v(k)$ and $C_v(k)$ were derived on-ground for time t_k as:

$$\begin{aligned} S_v(k) &= \sin(\Omega_d t_k) \\ C_v(k) &= \cos(\Omega_d t_k) \end{aligned} \qquad [8.11]$$

with the propagation coefficients:

$$\begin{aligned} S_d &= \sin(\Omega_d \Delta t) \\ C_d &= \cos(\Omega_d \Delta t) \end{aligned} \qquad [8.12]$$

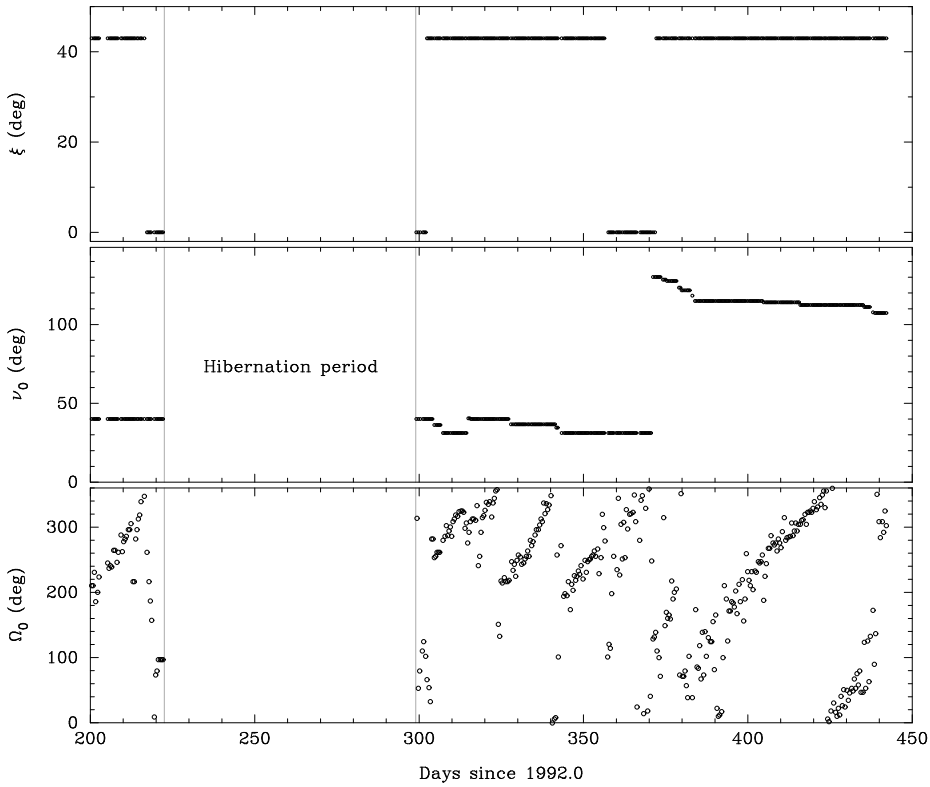

Figure 8.3. *Nominal scanning law parameters for the two-gyro operational phase. This phase occurred towards the end of the mission, following gyro failures which prevented continued three-gyro operations. The 'hibernation period' refers to an enforced period without scientific observations while the two-gyro operational mode was brought into service.*

$S_v(k), C_v(k), S_d, C_d$ were uplinked to the spacecraft and propagated on-board every Δt period as:

$$\begin{aligned} S_v(k) &= S_v(k-1)C_d + C_v(k-1)S_d \\ C_v(k) &= C_v(k-1)C_d - S_v(k-1)S_d \end{aligned} \qquad [8.13]$$

from which the nominal spacecraft body rates could be calculated:

$$\begin{aligned} \omega_X(t) &= \Omega_T S_v(k) \\ \omega_Y(t) &= \Omega_T C_v(k) \\ \omega_Z(t) &= \Omega_N \end{aligned} \qquad [8.14]$$

The on-ground orbital oscillator task was required to recalculate orbital oscillator values (S_v, C_v), propagation values (S_d, C_d) and transverse rate (Ω_T) and uplink these parameters to the spacecraft at regular intervals—nominally every 15 min—in both sun-pointing and normal modes. The orbital oscillator values calculated on ground corresponded exactly to the start time of a format on-board and were uplinked so that the new values were available on-board at precisely that time. The propagation values and transverse rate were less time-critical and were uplinked to be available on board shortly after the orbital oscillator values.

Uplink was performed automatically from ground through the mission planning system, although additional manual commanding was available if necessary. If for any reason, there was an interruption to commanding, there was no need to perform any emergency uplink of the orbital oscillator parameters since the on-board real time attitude determination showed no deterioration if the nominal scanning law rates were refreshed every hour or longer.

8.2. Star Observations

The star observing strategy algorithm, implemented in the on-board computer, made a selection, at regular time intervals, from the programme stars which crossed the field of view (information about the stars expected to cross the fields of view, on the basis of the nominal scanning law, was uplinked from the ground station to the satellite at regular intervals). The star observing strategy determined those stars that had to be observed, and allocated to them appropriate observation times.

The choice of the algorithm depended on optimisation criteria related to the performance of the mission, and on system constraints due to the hardware environment in which the star observing strategy had to operate. The main optimisation criteria were the following:

(1) minimisation of jitter effect: since observations of stars in the combined field of view were not strictly simultaneous, the attitude jitter of the satellite could introduce considerable noise in the measurements. The star observing strategy had to be able to minimise this effect by proper interlacing of star observations;

(2) distribution of observations between two viewing directions: implicit in the measurement concept was the capability of measuring relative angular distances between stars located far apart on the celestial sphere. It was one of the objectives of the star observing strategy to make sure that, when several stars were present in the combined field of view, angular distances were measured, whenever possible, between stars coming from the different fields of view;

(3) compatibility with the overall observing programme: in order to achieve the target precision at the end of the mission, stars of the various classes of magnitudes should have received, on average, a certain, predefined, global observation time. One of the functions of the star observing strategy was to ensure that stars received, during their crossing of the fields of view, a time allocation compatible with their global observation time;

(4) special emphasis on the observation of bright stars: observations of bright stars ($B < 9.0$ mag) were particularly valuable. Their positions could be measured with high precision, and these were subsequently used in the determination of the attitude of the satellite during the relatively long time periods (400 s on average) between attitude control jet firings. This ‘smoothing’ of the attitude determination provided, in turn, connections between pairs of bright stars not simultaneously present in the combined field of view. These additional connections considerably improved the final astrometric results. The star observing strategy was implemented such that bright stars were observed over as much of the scan as possible, i.e. as soon as they entered the field of view and until just before they left it;

(5) minimisation of errors due to grid imperfections: imperfections in the manufacture of the grid could induce errors in the phase measurements of a star. These errors were considerably reduced by a proper choice of the observation scheme.

The main system constraints related to the hardware environment in which the star observing strategy had to operate were the memory and time limitations of the on-board computer; the synchronisation with the telemetry format, the attitude and orbit control system, and the cold gas thruster firing; and constraints due to the downlink telemetry resources.

The Star Observing Strategy

The star observing strategy algorithm was built around a rigid time hierarchy and its operation was driven by three star-dependent parameters uplinked from ground. The time hierarchy was based on the following definitions:

(1) the sampling period, $T_1 = \frac{1}{1200}$ s, was the sampling time during which photoelectron counts were accumulated by the image dissector tube;

(2) the instantaneous field of view repositioning period, $T_2 = 8T_1 = \frac{1}{150}$ s, was the shortest time interval (or 'slot') during which the instantaneous field of view remained pointed on a given star. Each star was always observed for an integer number of slots, and the instantaneous field of view remained pointed at the same location on the grid throughout a slot. If a star was observed for more than one slot, the position of the instantaneous field of view was updated for the next slot;

(3) the interlacing period, $T_3 = 20T_2 = \frac{2}{15}$ s, was the period of time during which a group of up to 10 stars were observed;

(4) the observation frame period, $T_4 = 16T_3 = 2.133\ldots$ s, was the period of time during which essentially the same group of stars were observed in the same order and with a given observation time allocation (exceptions are discussed below);

(5) the transit time, $T_5 = 9T_4 = 19.2$ s, was roughly the time interval taken for any given star to cross one of the fields of view of the telescope.

Star-Dependent Parameters

The star-dependent parameters uplinked from ground, and on which the star observing algorithm operated, were:

(1) the selection index: the parameter used to calculate the priority with which a programme star must be observed with respect to the other programme stars simultaneously present in the field of view;

(2) the minimum observation time: the minimum number of slots of T_2 which, at frame level, had to be allocated to a star in order to achieve a sufficient precision in phase extraction (this was a function of the magnitude of the star);

(3) the target observation time: the observation time which, at frame level, had to be allocated to a given star in order to achieve, at the end of the mission, the global observation time associated with that star (this was also a function of the magnitude of the star).

The values of the star-dependent parameters could vary during the mission, to take into account the past and projected observational history of the star, but they were fixed during each crossing of the field of view by the star. The values of the minimum and target observation times for a star of given magnitude were determined on the basis of simulations carried out by the INCA Consortium and the data reduction consortia, and were uplinked during the mission from ESOC to the satellite, where the star observing strategy was implemented.

Other parameters included in the star observing strategy algorithm were: the predicted time of entrance of the star in the field of view; its magnitude; a flag indicating whether the star was observed in the preceding or following viewing direction; and a flag indicating whether the star should have been observed by the star mapper for attitude-measurement purposes (a subset of some 40 000 programme stars, in particular bright stars with good *a priori* positional accuracies, fell into this category).

During the operations, ESOC processed the data derived from the Hipparcos Input Catalogue and the observational history of the programme stars to produce a so-called 'programme star file', which contained the information to be uplinked to the satellite. The programme star file contained star identifications, magnitudes, field of view entering times, viewing direction flags (the transverse coordinate needed for detector piloting and real-time attitude estimation), and the current values of the three star-dependent parameters discussed above. A scheme for the data processing involved in the generation of the programme star file is shown in Figure 8.4.

Fully and Partially Observable Stars

When a frame of $T_4 = 2.133\ldots$ s was considered, stars that remained in the combined field of view during the entire frame were called fully observable stars; those that remained in the combined field of view only for a part of the frame, but not less than three interlacing periods ($3T_3$), were called partially observable stars—these could be stars that either left or entered the combined field of view during the frame period.

One way to visualise the flow of programme stars in and out of the combined field of view is by means of a time diagram, such as that shown in Figure 8.5. A star S_i entered the field of view at time t_0^i and left it at time $t_0^i + T_5$. The 'transit line':

$$f_i(t) = \frac{t - t_0^i}{T_5} \qquad [8.15]$$

represents the fraction of transit time spent by the star in the field of view:

$$0 \le f_i(t) \le 1 \qquad [8.16]$$

The stars that were present in the field of view at a given time t' could easily be identified by drawing the line $t = t'$: they are those whose transit lines are intercepted by $t = t'$.

By marking on the t-axis the time intervals corresponding to subsequent frames of $T_4 = 2.133\ldots$ s, one can also identify the stars present in a given frame. For example, in frame number 10 of Figure 8.5, there are three stars present in the combined field of view, of which two are fully observable stars and one is a partially observable star, leaving the field of view before the end of the frame period.

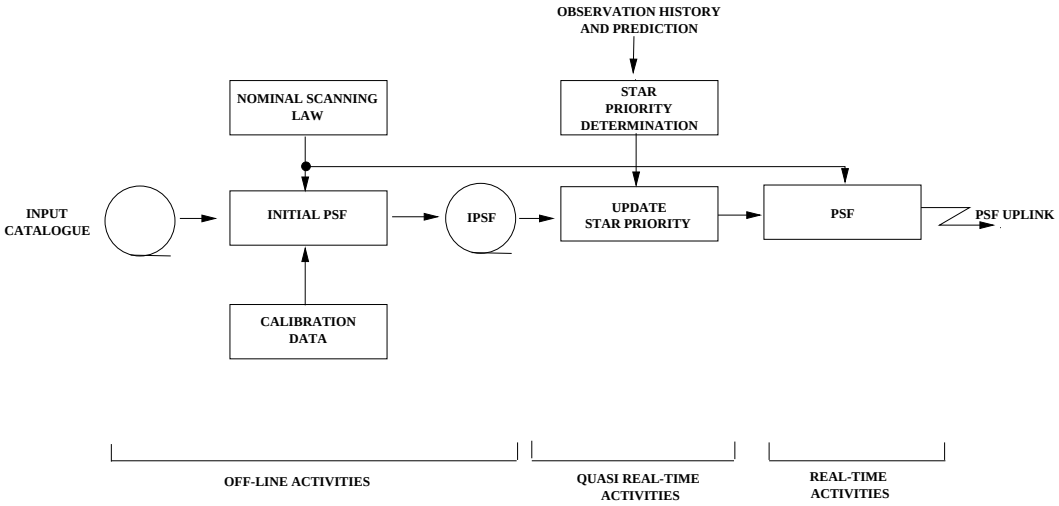

Figure 8.4. *Data processing involved in the generation of the programme star file (PSF).*

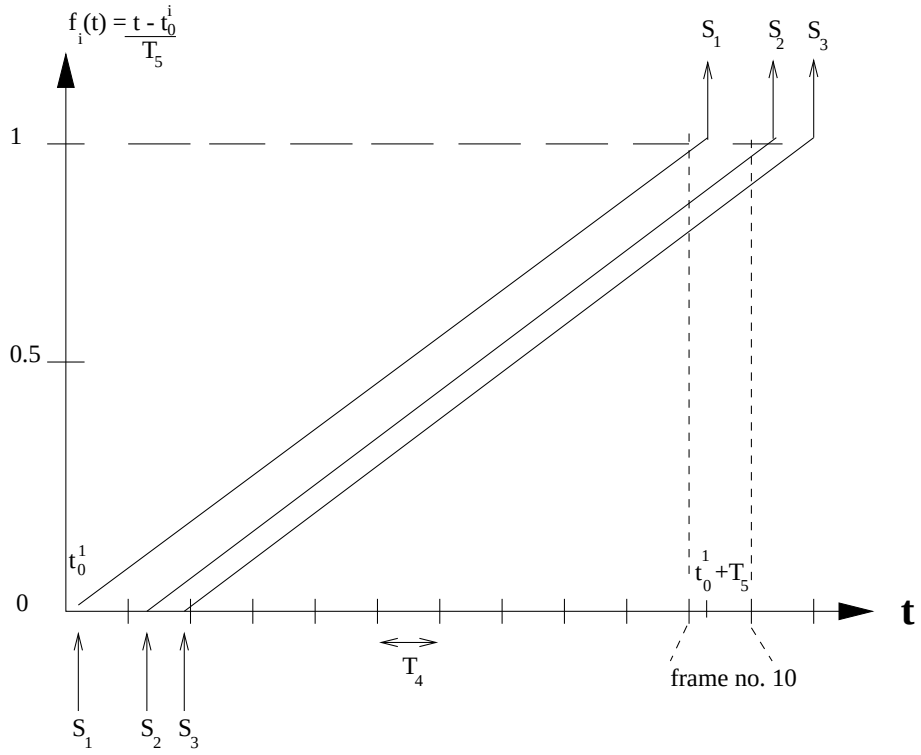

Figure 8.5. *The flow of programme stars in and out the combined field of view, illustrated by means of a time diagram. Stars S_1, S_2, S_3 enter the combined field of view at the bottom left of the diagram, and exit at the top right. An observation frame extends over an interval of T_4 (2.133 . . . s). See text for details.*

Star Selection

The star observing strategy algorithm involved both star selection and observation-time allocation. Star selection proceeded according to the following rules:

(1) from the data contained in the programme star file and the real-time attitude calculated on-board, the stars present in the combined field of view for the next frame were identified; the first 15 of them were retained for further selection;

(2) among the stars retained, the partially observable stars were identified and classified into 'leaving' and 'entering' stars;

(3) the fully observable stars were identified;

(4) if there was at least one fully observable star, up to two partially observable stars were selected (one leaving and one entering) provided that they were brighter than magnitude $B = 9$ mag, choosing the brightest in each class;

(5) if there was no fully observable star, up to two partially observable stars were selected (one leaving and one entering) choosing the brightest in each class;

(6) once the partially observable stars, if any, were selected, the selection of the fully observable stars proceeded as follows: (a) alternatively one star was selected from the preceding and one star from the following viewing direction, until one of the two groups was exhausted; then the remaining stars were added; (b) within each of the two groups, stars were selected according to their priority index, defined by:

$$P_i = (-1)^k \frac{t_k - t_0^i}{T_5} b_i \qquad [8.17]$$

where i is the star identification number of star S_i, k is the frame identification number, t_0^i is the time of entrance of star S_i in the field of view, t_k is the mid-time of frame k, b_i is the selection index, and T_5 is the transit time. Priority was then given to stars with the higher values of P_i. Due to the factor $(-1)^k$, priority indices changed sign from one frame to the next, in such a way that priorities alternated: the star with the highest priority in frame k was, as a rule, the star with the lowest priority in frame $k + 1$;

(7) the complete list of selected stars consisted of the partially observable stars, if any, plus a number of fully observable stars, if any, such that the total number of stars selected for observation during the relevant frame period did not exceed ten. The alternating priority parameter ensured that, in those (rare) cases where more than 10 stars were simultaneously visible in the combined field of view, those stars not observed during one frame period were observed during the subsequent frame.

Observation Time Allocation

Observation time was allocated over an interlacing period of $T_3 = \frac{2}{15}$ s. The resulting time allocation was repeated for the 16 interlacing periods contained in a frame, except for the change described at point (5) below. The observing time was allocated as follows:

(1) if there was no fully observable star in the field of view, 10 slots of $T_2 = \frac{1}{150}$ s were allocated to each partially observable star when two partially observable stars were

selected, or all 20 slots of T_2 to the one partially observable star, if only one partially observable star was selected;

(2) if there was at least one fully observable star in the field of view, two slots were allocated to each partially observable star selected. Once the observation time allocation to partially observable stars was completed, the remaining slots available were allocated to the selected fully observable stars as follows:

(3) each fully observable star was allocated, in sequence, its minimum observation time, until either the list of stars was exhausted or the number of slots available (20) in the interlacing period was exceeded. In the latter case, the remaining fully observable stars were dropped from the observation list and no longer considered. In the absence of any partially observable stars, at least two fully observable stars, if present, would always be observed, by allocating, if necessary, an observation time shorter than the minimum observation time (for the faintest stars the nominal minimum observation time was larger than 10 slots);

(4) the remaining slots, if any, were allocated one by one to the fully observable stars actually observed, on the basis of their so-called 'performance index' z_i, defined as:

$$z_i = \frac{n_i}{\underline{t}_i} \qquad [8.18]$$

where n_i is the actual number of slots which had already been allocated to the star in the interlacing period, and $\underline{t}_i$ is the target time. The first available slot was allocated to the star with the lowest performance index, and so on;

(5) if a partially observable star was actually observed, the 2 slots which were free when the star was *not* present in the field were allocated to the fully observable star with the lowest performance index—referred to below as its 'associated' fully observable star.

Execution of the Observing Sequence

The observation sequence was then executed in the following order:

(1) in each interlacing period fully observable stars were observed in order of entry;

(2) all slots devoted to the same star were contiguous;

(3) during the interlacing periods in which partially observable stars were present, the observation slots of each partially observable star were contiguous with the ones of its associated fully observable star;

(4) the entering partially observable star was observed after its associated fully observable star;

(5) the leaving partially observable star was observed before its associated fully observable star;

(6) if there was no fully observable star, the leaving partially observable star was observed before the entering partially observable star.

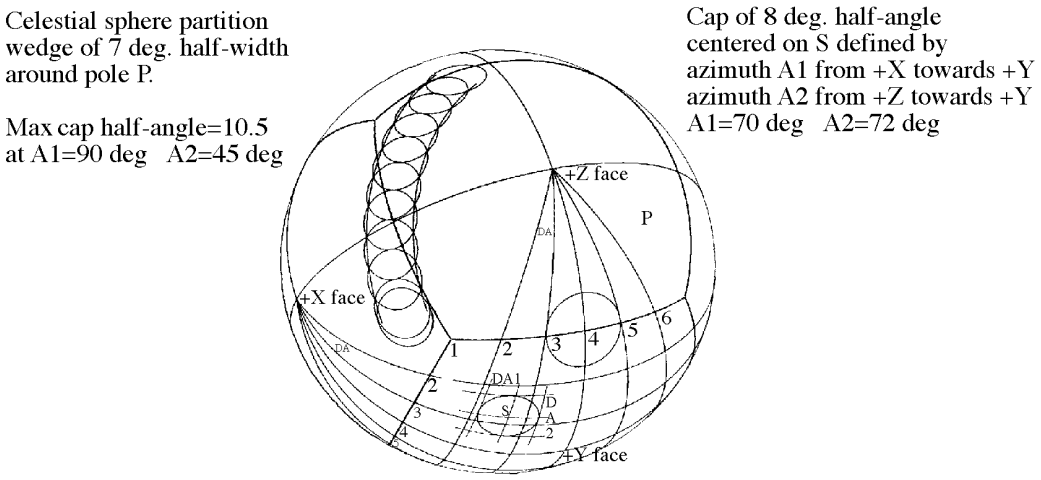

Figure 8.6. *Partitioning of the celestial sphere for the operational Hipparcos Input Catalogue implemented at ESOC.*

8.3. Input Catalogue Consortium Interfaces with ESOC

The Hipparcos Input Catalogue contained all relevant data for the 120 000 programme stars to be observed by the satellite. The stars chosen for the Hipparcos Input Catalogue fulfilled complex selection criteria related primarily to their scientific interest, but also taking into account other factors, such as their magnitude, their distribution over the entire sky, their proximity to other bright objects, and their role in the satellite attitude control and in the data processing. All these properties were then used to optimise the planned observation sequence obtaining the most homogeneous set of observations of objects on the entire sky over the lifetime of the mission.

The INCA Consortium provided ESOC with the main Hipparcos Input Catalogue, and a number of annexes including information on: (i) double and multiple stars; (ii) ephemerides for large-amplitude variable stars; (iii) approximately 13 000 additional stars with $B < 9.0$ mag not contained in the catalogue of programme stars but which were included as real-time attitude determination guide stars to provide more uniform sky coverage for the attitude control.

From the main catalogue ESOC generated an operational version which was partitioned according to a 'celestial cube' structure to ensure a fast access time. Conceptually the celestial sphere was first divided into six identical parts corresponding to the faces of a cube inscribed into the sphere. Each face was further divided into elementary zones of approximately $3° \times 3°$ by a grid of mutually orthogonal great circles (Figure 8.6). The main operational catalogue was augmented by an index file which contained a restricted set of data for each star, namely the position, magnitude, and HIC (Hipparcos Input Catalogue) number. The stars were ordered within the index file according to zone, the HIC number providing the key to the main catalogue.

In deriving the operational input catalogue various other parameters were computed, including, (a) variability flags, (b) target observation times, (c) lower and upper minimum observation times, (d) accuracy test vectors and (e) initial covariance matrices for the modulation strategy. The target observing time, $\underline{t}$, represented the mean time a star should be observed when crossing one of the fields of view. It was derived from the overall target time T (for the entire mission) and the average number $N(\beta)$ of crossings throughout the mission, where β was the ecliptic latitude of the star, and was given by:

$$\underline{t} = T / N(\beta) \qquad [8.19]$$

where T (in seconds) was a function of the Hipparcos magnitude (Hp):

$$\begin{aligned} T &= -750 + 560Hp - 89.5Hp^2 + 4.88Hp^3 \quad (Hp > 5.0) \\ T &= \ \ 420 \qquad\qquad\qquad\qquad\qquad\quad (Hp \leq 5.0) \end{aligned} \qquad [8.20]$$

$N(\beta)$ was derived by interpolation from Table 8.2.

Hipparcos Input Catalogue Updating

As the data reduction consortia processed the science data, more accurate positions were determined for the catalogue stars. These results were made available to ESOC for use in the programme star file, thereby improving the overall accuracy, not only of the instantaneous field of view positioning, but also of the real-time attitude determination performance, which in turn led to further improvements in overall mission accuracies. In addition, a small number of star positions and magnitudes had to be corrected at the start of the mission. Table 8.3 provides a summary of the principal catalogue updates carried out at ESOC during the mission.

Variable Star Ephemerides

Large-amplitude variable stars required special consideration since, to optimise observing time, it was important to be able to predict their apparent magnitudes. This was done by using specific variable star ephemerides, provided by the INCA Consortium. Once a variable star had been observed by the satellite, the data was processed at ESOC and the results were communicated back to the INCA Consortium, once per month, to further refine the ephemerides. Periodically, a new version of these ephemerides was sent to ESOC for use in generating the programme star file (see Table 8.3).

ESOC processed the observations of variable stars in two stages: (i) payload monitoring, performed in near real-time, and (ii) payload reporting, running off-line. The payload monitoring software is described in detail in Chapter 10. Every 60 s, the program selected one star observed in the preceding 30 s. The selection criteria were heavily weighted in favour of the large-amplitude variable stars, so that if one was present in the interval it was invariably selected for processing.

The second payload reporting program ran daily on the off-line main-frame computer at ESOC processing the previous 24 hours of payload monitoring results, and compiling statistics on various aspects of the general results. In addition, a longer run was performed every week specifically to obtain the large-amplitude variable star results.

Table 8.2. Mean scanning frequency as a function of ecliptic latitude.

$\lvert\beta\rvert$	0	10	20	30	40	47	55	65	75	85	90
$N(\beta)$	120	124	134	148	190	280	200	164	150	146	146

Piloting and Magnitude Monitoring

The main reason for running payload reporting every 24 hours was to obtain information concerning the intervals when image dissector tube piloting was 'good' in some sense. The intervals of 'good', 'bad' and 'unknown' image dissector tube piloting were used by the FAST and NDAC Consortia who only processed data when piloting was 'good'. A history of the piloting throughout the mission was held on a sequential file on the IBM main-frame. The information was also used by the observation modulation strategy software which updated observation priorities in the newly generated programme star file given the previous history of observations.

'Good' piloting was defined to be when the last three payload monitoring reports from both fields of view, showed agreement between predicted and measured *Hp* magnitudes to within 1.5 mag. 'Bad' piloting was defined to be when three consecutive payload monitoring reports from one field of view disagreed by more than 1.5 mag in their predicted and measured *Hp* magnitudes. 'Unknown' piloting was defined when there were no payload monitoring reports for over 45 min (usually during loss of signal around perigee). Piloting status flags in the telemetry data stream switched when any of these conditions were satisfied.

This piloting information was incorporated into the variable star reports which were generated in the weekly runs of payload reporting. The main processing steps within the payload reporting task which were relevant for variable star processing and image dissector tube piloting determination were:

(1) each payload monitoring record in the prescribed interval was extracted from the history file (normally extending some 20 days in the past);

(2) the predicted *Hp* magnitude was extracted from the input catalogue for the non-variable stars. For the variable stars the predicted *Hp* magnitude was calculated by linear interpolation from the ephemerides (data points separated by 10 days);

(3) the image dissector tube piloting at the time of observation was extracted from the piloting file if the data was available from previous results from payload reporting;

(4) the measured *Hp* magnitude was calculated (as described below). A record was written to the variable star report file containing the following information:
   - time of on-board observation;
   - Hipparcos Input Catalogue (HIC) identifier of monitored star;
   - blue magnitude of star;
   - colour of star;
   - sample count, i.e. observation time in units of 1/1200 s;
   - quality of preceding observation (see Chapter 10);
   - quality of image dissector tube piloting;

- field of view indicator (1 for preceding, 2 for following);
- observed intensity, I_0 in counts per s;
- measured modulation coefficient M_1;
- measured modulation coefficient M_2;
- predicted Hp magnitude;
- measured Hp magnitude;
- the difference between the predicted and measured Hp magnitudes.

The measured Hp magnitude as calculated above was dependent on (i) the measured count rate I_0; (ii) the field of view, $\epsilon = +1$ (preceding field of view), $\epsilon = -1$ (following field of view); (iii) the coordinates of the star on the main grid (G, H), and (iv) the colour index of star, $c = B - V - 0.5$.

A calibration of the transformation between measured count rates and Hp magnitude was conducted routinely by the FAST Consortium's 'first-look' facility at Utrecht. The calibration was performed using a least-squares fit, for photometric standard stars only, to the 17 unknown coefficients r_i in the following equations:

$$R = r_0 + r_1\epsilon + r_2 I_0 + r_3 I_0^2 + r_4 G + r_5 H + r_6 G^2 + r_7 GH + r_8 H^2 + r_9 G^3 + r_{10} G^2 H + r_{11} GH^2 + r_{12} H^3 + r_{13} c + r_{14} c^2 + r_{15} cG + r_{16} cH \quad [8.21]$$

and:

$$I_C = I_R \, R \, 10^{0.4(9-Hp)} \quad [8.22]$$

where I_C is the corrected value of I_0 for a star of Hipparcos magnitude Hp and I_R is a reference intensity for a star of magnitude $Hp = 9$ mag. ($I_R = 1760$ for the image dissector tube used throughout the mission). With I_R known and R calculated, the Hipparcos magnitude was given by:

$$Hp = 9 - 2.5 \log_{10}(I_0/(I_R R)) \quad [8.23]$$

Minor and Major Planet Ephemerides

In addition to the stars defined in the Hipparcos Input Catalogue, several solar system objects were contained within the original observing programme: 48 minor planets; the Jovian moon, Europa; and the Saturnian moon, Titan. In order to schedule these objects within the programme star file, accurate ephemerides for the major and minor planets were provided by the Bureau des Longitudes. These ephemerides were updated on a regular basis. In addition, a further Saturnian moon, Iapetus, was added to the observing programme part way through the mission. It had been expected that the Moon's brightness and separation from Saturn would make it a difficult candidate for observation. Nevertheless, the payload proved to be sufficiently sensitive to be able to make a series of good observations.

One other object which was added after the mission was started was the quasar 3C 273. This object, always considered to be at the very limit of the satellite's observational capabilities, was added in view of its possible role in defining an inertial reference system. As expected, however, the observations of this object provided very little additional weight in this respect.

Table 8.3. History of principal catalogue updates at ESOC.

Date	Description
01/12/89	Hipparcos Input Catalogue Version 6
20/12/89	Variable Star Ephemerides
23/03/90	Variable Star Ephemerides
21/06/90	Minor Planet Ephemerides
04/07/90	Hipparcos Input Catalogue Version 7
04/07/90	Variable Star Ephemerides
27/10/90	Variable Star Ephemerides
22/01/91	Variable Star Ephemerides
21/02/91	Hipparcos Input Catalogue Version 8
21/04/91	Hipparcos Input Catalogue Version 9
03/07/91	Minor Planet Ephemerides
03/07/91	Variable Star Ephemerides
06/08/91	Major Planet Ephemerides
06/08/91	Minor Planet Ephemerides
22/11/91	Europe, Titan, Iapetus Ephemerides
19/03/92	Variable Star Ephemerides
01/12/92	Hipparcos Input Catalogue Version 10
30/11/92	Minor Planet Ephemerides
16/12/92	Europe, Titan, Iapetus Ephemerides

History of Hipparcos Input Catalogue Updates during Operations

Table 8.3 lists the main updates which were made to the various catalogues and ephemerides throughout the mission. Versions 1 to 5 of the Hipparcos Input Catalogue were implemented at ESOC before launch. Smaller incremental changes were occasionally made at other times.

8.4. Programme Star File Generation

Basic Methodology

To hold the complete Hipparcos Input Catalogue (with details of the 120 000 stars and other objects to be observed) on-board and implement the observation strategy described in the previous section would have imposed too much of a computational burden on the on-board computer. The solution was to hold only the relevant star observation parameters for the next 20–30 minutes, and to refresh it by regular commands from ground. This buffer was called the ‘programme star file’.

The programme star file contained star identifications, magnitudes, field of view entry times, field of view identifications and the observation strategy parameters discussed in the previous section. The observation duration was calculated taking into account the brightness of the star (the fainter the star the longer the observation), its scientific

priority, the number of other programme stars within the field of view competing for the available observing time, and the number of times the star had already been observed during the mission. Because there were long periods without ground station support, some stars were under-observed over a particular time interval. Consequently, the relative importance of observing these stars later was increased. In this way, all the stars in the catalogue were observed sufficiently to provide reasonably uniform accuracies in position, parallax and proper motion, by the end of the mission.

The off-line IBM mainframe at ESOC prepared an on-ground 'extended programme star file', from where it was transferred to the Hipparcos dedicated control system on the real-time VAX. The extended programme star file contained not only data required by the on-board programme star file, but also additional data required for the on-ground payload monitoring software.

During the routine operational phase, the extended programme star file was generated on a daily basis, then transferred and uplinked regularly. In the two- and zero-gyro operational phases, where the nominal scanning law parameters were varying after every perigee, the extended programme star file could only be generated once the new nominal scanning law parameters had been determined. A history of the latest two weeks of data was maintained to allow post processing for payload calibration activities and maintenance of the modulation strategy. The creation of the daily extended programme star file is summarised as follows:

(1) a coarse selection was made of objects which would cross the field of view in the given period. The basic principle was to calculate the nominal scanning law attitude at very close intervals of time and for each field of view extract from the star catalogue the stars which were in the vicinity of the pointing directions. For each candidate star, an accurate transit time and ordinate was computed. If the ordinate was within the allowed range a star transit record was generated. This selection procedure was made efficiently through the use of the partitioned operational input catalogue (see Section 8.3);

(2) as soon as a star had been selected in the coarse selection phase, its accurate transit time was computed, taking account of: (a) proper motion in ecliptic longitude and latitude, (b) parallaxes for nearby stars, and (c) stellar aberration due to the combined motions of the spacecraft around the Earth and the Earth around the Sun;

(3) observation parameters were computed for each object to be observed on the main grid. These observation parameters were the minimum observation time expressed in a number of slots per interlacing period and the target observation time expressed in a number of slots per frame (2.133... s). These two parameters were used by the on-board star observation strategy to share the observation time between the programme stars present in the combined field of view (see previous section). For programme stars, these parameters were derived from the initial values modulated by the current observation history, characterised by the covariance matrix B (described in Section 8.5). For variable stars and solar system objects the observation parameters were only a function of the current magnitude and the ecliptic latitude.

In addition to nominal programme star files, ESOC were responsible for generating the special programme star files to support the initial calibration activities (Chapter 5). These programme star files were classified into two categories: those derived from the nominal scanning law, but with special requirements on the stars to be observed (e.g.

star magnitude, star density) and those derived from a non-nominal scanning law (e.g. the non-nominal sun-pointing operations with solar aspect angle $\xi = 0$).

Mission planning products acted as input for the extended programme star file generation since the mission plan (generated on a weekly basis) provided the times of any special calibration, Earth and Moon occultations when one or both fields of view were obscured, and ground station outage when a sparse programme star file was required (see below). A fuller description of the mission planning system is given in Section 4.6.

Real-Time Attitude Determination Guide Stars

Approximately 60 per cent of all programme stars were selected as guide stars for the on-board attitude control. The conditions for selection were that (a) the star had a variability range less than 0.02 mag; (b) its B_T magnitude was in the range 5.0–9.5 mag; and (c) its position accuracy was better than 0.8 arcsec. A component of a double or multiple star system could be selected if certain additional conditions were satisfied: (a) the distance to other components was larger than 23 arcsec; or (b) the difference in magnitude was larger than 1.5 for separations between 0.8 and 23 arcsec; or (c) for a separation not exceeding 0.8 arcsec, the root-mean-square of the separation and position accuracy did not exceed 0.8 arcsec.

Sparse Programme Star File

Significant modifications to the programme star file generation software were necessary for the revised mission. With the revised elliptical orbit, non-coverage periods lasting several hours were occurring routinely. Particularly, during the first months of the revised mission, before two further ground stations were made available on a regular basis, complete orbits were without coverage at times. Given that there was only sufficient memory for a nominal programme star file to last for about 20–30 min, real-time attitude determination would have diverged within a few minutes of the end of the programme star file. For an extended loss of coverage lasting 10 hours, the attitude of the spacecraft could have deviated from the nominal scanning law sufficiently to cause the on-board emergency sun acquisition mode to trigger.

This prompted the development of the so called ‘sparse programme star file’ for non-coverage periods to ensure permanent convergence of real-time attitude determination. This sparse programme star file consisted of only the brightest reference stars, spanning the non-visibility periods of up to 12 hours, thus providing continuous information for the attitude control system between two successive stations’ support.

Alternating Strategy

On 20 September 1991, the programme star file generation software was revised to include an alternating selection strategy for stars in the open cluster NGC 2516, where four stars in a small region of the sky were added to the programme to serve as calibration objects for the Fine Guidance Sensors on-board the Hubble Space Telescope.

Straightforward inclusion of these stars was not possible, as they exceeded the programme star file requirements for adequate observation time for each object. The solution was to allow approximately half the objects to be observed during one rotation

period of the spacecraft, then to allow those which were not observed in the previous period to be observed in the following. Subsequent scans across this area of the sky resulted in alternating selections of stars within the programme star file.

8.5. Modulation Strategy

Target observing times defined in Section 8.2 had been defined initially in order to achieve, as far as possible, uniform accuracy of the final Hipparcos astrometric data over the whole celestial sphere assuming nominal scanning. At the start of the mission, in order to fix those target times, it was necessary to compute, for each programme star, the 5×5 target covariance matrix, B, of the five astrometric unknowns (the ecliptic longitude and latitude, the ecliptic components of proper motion, and the parallax) based on the nominal scanning law. The memory of those target covariances was kept throughout the mission, while actual covariances were obtained via the routine updating process defined below. This process was equivalent to substituting each day in matrix B the actual observing times compared with the target ones. Comparing actual to target variances indicated whether stars were running under- or over-observed with respect to plans. Star-dependent parameters were then modified in the programme star file in order to give highest priority to the most important observations occurring over the coming hours.

The computation of the initial matrix B was performed at ESOC after receiving the main catalogue from the INCA Consortium. The most computationally efficient method to do this was to compute the matrix for each star in sequence, calculating all expected transit times over the predicted mission duration. The following steps were performed for each programme star:

(1) the information matrix $A(5,5)$ was initialised to zero;

(2) on the assumption that the parameters defining the nominal scanning law were fixed throughout the mission, the precession rates and rotation rates were used to extrapolate from the last observation to the next observation time. The use of the transit time was limited to the derivation of the inclination angle, i, which was defined to be the angle between the scan direction and the local ecliptic meridian at the time of observation. It followed that the level of accuracy was not as stringent as in the case of programme star file generation. In particular the effects of proper motion, parallax and aberration were neglected. It was however necessary to check whether the star crossed one or both fields of view setting n_i to 1 or 2 accordingly;

(3) for each transit, the five observation coefficients $a(1) \ldots a(5)$ were computed as follows. Defining:

(λ, β) as the star ecliptic longitude and latitude

λ_s as the sun ecliptic longitude

(X_0, Y_0, Z_0) as the orientation of the scan axis

T_i is the computed transit time (years)

T_0 is the expected mission mid-point time (years)

μ_s is the drift angle of the star (radians)

Then:

$$\cos i = X_0 \sin\lambda - Y_0 \cos\lambda$$
$$\sin i = \pm\sqrt{1 - \cos^2 i} \qquad [8.24]$$

where $\sin i$ takes the sign of Z_0. Finally:

$$\begin{aligned} a(1) &= \sin i \\ a(2) &= \cos i \\ a(3) &= (T_i - T_0)\sin i \\ a(4) &= (T_i - T_0)\cos i \\ a(5) &= \sin(\lambda_s - \lambda)\sin i - \cos(\lambda_s - \lambda)\cos i \cos\beta \end{aligned} \qquad [8.25]$$

(4) the information matrix was then updated using the number of observations n_i in the current revolution period, and the target observing time $\underline{t}$:

$$A(j,k) = A(j,k) + a(j)a(k)n_i\underline{t} \qquad [8.26]$$

(5) the symmetric matrix A was inverted to derive the covariance matrix B.

Routine Updating

Since the target observing time was derived from the covariance matrix of observations as available for each star in the main catalogue, the main catalogue at ESOC had to be updated on a daily basis taking account of the telemetered image dissector tube observation reports since the previous processing run. The processing of the image dissector tube observations was scheduled automatically on the off-line mainframe computer at ESOC. Again, this procedure only applied to the non-variable programme stars; solar system objects were not considered. The sequence of events was as follows:

- the image dissector tube reports were retrieved from the archive files on the front-end dedicated computer system and transferred to the off-line machine;
- the programme star file star identifiers (running from 0 to 255) were correlated with the HIC identifier in the extended programme star file, using the expected and observed transit times;
- the reports were archived and sorted according to HIC number;
- the total accumulated observation time was computed for every star each time it crossed one of the fields of view;
- the covariance matrices in the input catalogue records were updated according to the total observation times;
- a record was maintained of the last image dissector tube report to be successfully processed to allow the next processing run to continue from the correct time.

In order to update a covariance matrix, the HIC number in the (ground-based) extended programme star file record was used to extract the corresponding input catalogue record. The new covariance matrix was then computed using the old covariance matrix, the total observation time in this processing interval as well as certain additional data contained in the extended programme star file record.

Defining:

t_{obs} as the total accumulated observation time for the star in question as it transited a field of view

$\underline{t}$ as the target observing time per field of view transit (defined in the previous section)

$\vec{a}$ as the five observation coefficients, $a(1) \ldots a(5)$

B as the covariance matrix

Then B was updated using the following equations:

$$\begin{aligned} s &= \text{sign}(\underline{t} - t) \\ \vec{o} &= \sqrt{|\underline{t} - t|}\vec{a} \\ \vec{u} &= B\vec{o}^T \\ c &= -s\vec{o}\vec{u} + 1 \\ B &= B + \frac{s}{c}\vec{u}.\vec{u}^T \end{aligned} \qquad [8.27]$$

Consequences for the Revised Mission

On 9 May 1990, the revised observation modulation strategy taking account of the revised mission profile, was implemented within the flight dynamics system at ESOC. Significant revision to the strategy was necessary in order to account for long periodic losses of signal and loss of real-time attitude determination convergence around perigee when computing the initial covariance matrices, as follows:

(1) re-computation of the initial covariance matrix. The observation time which would be lost for each star due to perigee passage, ground station outages, occultations by the Moon and the Earth, and consequent loss of good measurements could not be predicted accurately over the projected 2.5 years of the revised mission. A coarse estimate was made of the loss, estimated to be between 20 and 30 per cent, depending on the ecliptic latitude of the star. For each star of the programme the overall target time T (see Section 8.3) was modified accordingly and the initial covariance matrix recomputed as a function of all nominal transits over the mission duration;

(2) recording of good observation periods. In the initial implementation of the modulation strategy it was assumed that all measurements would be of good quality. Access to the telemetry was required only to find how much time was effectively devoted to the observation of a star for a particular transit. In the actual mission the real-time attitude determination on-board diverged frequently mainly during perigee passage. This led to bad piloting of the image dissector tube and hence useless star measurements. The detailed time allocation recorded in the telemetry star observation reports was then of no value. Fortunately times of good observation periods could be provided by an already existing payload reporting program, running off-line on a daily basis (see Chapter 10). The modulation strategy package was modified to interface with this program, thus having access to the periods of ‘good’, ‘bad’ and ‘unknown’ piloting quality.

Results

Current values of the observation parameters were regularly communicated to the INCA Consortium for cross-checking that the modulation strategy was producing optimised observing times. Performance assessments made in May 1991 and March 1992 showed that the revised modulation strategy worked according to expectations. A detailed report of the May 1991 assessment study was given in Crézé & Chareton (1991). In particular

some stars which had been drastically under-observed in the early part of the mission slowly recovered the accuracy expected later in the mission as a result. The modulation strategy was eventualy switched off towards the end of 1992 when it became clear that no reliable long-term prediction of the nominal scanning law could be given in view of the gyro failures and consequent attitude control problems.